Macromolecules

pubs.acs.org/Macromolecules Article

Polymer Tacticity Effects in Polymer–Lanthanide Chelation Thermodynamics

William R. Archer, Taoyi Chen, Valerie Vaissier Welborn, and Michael D. Schulz*

Cite This: *Macromolecules* 2023, 56, 9062–9069 Read Online

ACCESS | Metrics & More | Article Recommendations | Supporting Information

ABSTRACT: Metal-chelating polymers are critical components in numerous applications. However, despite the known influence of polymer tacticity on both bulk and solution properties, most materials used in metal-chelation applications are atactic. Here, we investigate the relationship between polymer tacticity and polymer–lanthanide interactions in aqueous solution. We synthesized a series of five poly(methacrylic acid)s with systematic variations in tacticity (20–99% *m* diads) and used isothermal titration calorimetry to measure the thermodynamics of lanthanide binding to each material (ΔH, ΔG, ΔS, K_a, and stoichiometry). We observed enthalpy–entropy compensation across this tacticity series, finding that both $|\Delta H|$ and $|\Delta S|$ decreased with decreasing *m* diad content while ΔG remained similar. Molecular dynamics simulations of the polymer–metal interactions revealed that the observed differences in binding thermodynamics may be largely ascribed to differences in polymer flexibility. These combined experimental and computational results demonstrate that metal binding can be influenced by altering the polymer stereochemistry, ultimately influencing the design of more efficient metal-chelating materials.

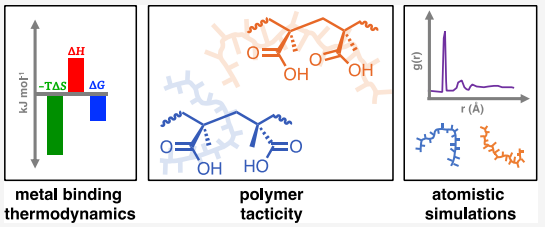

INTRODUCTION

The stereochemistry of natural and synthetic macromolecules frequently dictates their higher-order structure and function.[1−4] In proteins, stereoregularity often facilitates conformational changes in response to solution conditions,[5,6] metal binding,[7] or chemical modification.[8] Similarly, the properties of synthetic polymers are directly linked to tacticity.[9−15] For example, the glass-transition temperatures (T_g) of isotactic and syndiotactic poly(methyl methacrylate)[16] differ by almost 81 K, and similar differences are observed for tactic poly(acrylic acid)[17] and polystyrene.[18] Tacticity effects also appear in solution, e.g., isotactic poly(methacrylic acid) (PMAA), is a weaker acid than syndiotactic PMAA due to increased charge repulsions along the polymer backbone when the carboxylates are oriented in the same direction.[19] This connection between tacticity and material properties extends to metal-chelating polymers as well.[20]

Metal-chelating polymers have been investigated for myriad applications including toxic metal contaminant removal, radionuclide delivery for cancer treatment, and recovery of valuable metals from waste streams.[21−24] Rare-earth elements (REEs: Y, Sc, La–Lu)[25] are one such class of valuable metals as they are critical components in many technologies such as wind turbines (Nd and Dy) and light-emitting diode light bulbs (Eu, Tb, and Y).[26−29] As demand for REEs outpaces supply, new and sustainable sources of REEs are needed as well as more efficient methods of extraction and purification. Polymers often play a central role in developing novel approaches to REE production, and materials containing carboxylates,[30] phosphonates,[31] or sulfonates[32] have proven particularly useful in REE extraction applications. Thus, quantifying polymer structure–property relationships is critical to guiding the development of future REE-chelating materials. Previous work by Okamoto and co-workers demonstrated that Tb^{3+} bound more strongly to an isotactic trimer model of poly(acrylic acid) than the analogous syndiotactic trimer.[33] These results indicated that Tb^{3+} complexation first involves the nearest carboxylate neighbors, followed by successive ligand complexation by the most geometrically favorable carboxylates. However, despite the known influence of small-molecule and polymer stereochemistry on metal binding,[33−37] virtually all the materials currently employed in metal-chelation applications are atactic.

Metal-chelating polymers often change conformation in response to metal binding,[38,39] and polymer conformation can be influenced by several factors, including stereochemistry.[40−43] For example, previous simulations of PMAA have indicated that *isotactic*-PMAA has a larger radius of gyration than *syndiotactic* PMAA, and exists in an extended-chain conformation at high degrees of neutralization.[44] Because the polymer conformation and polymer–metal binding are linked, we hypothesized that tacticity could be leveraged to modulate

Received: July 8, 2023
Revised: October 21, 2023
Accepted: October 30, 2023
Published: November 13, 2023

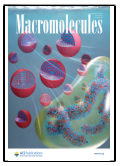

https://doi.org/10.1021/acs.macromol.3c01163
Macromolecules 2023, 56, 9062–9069

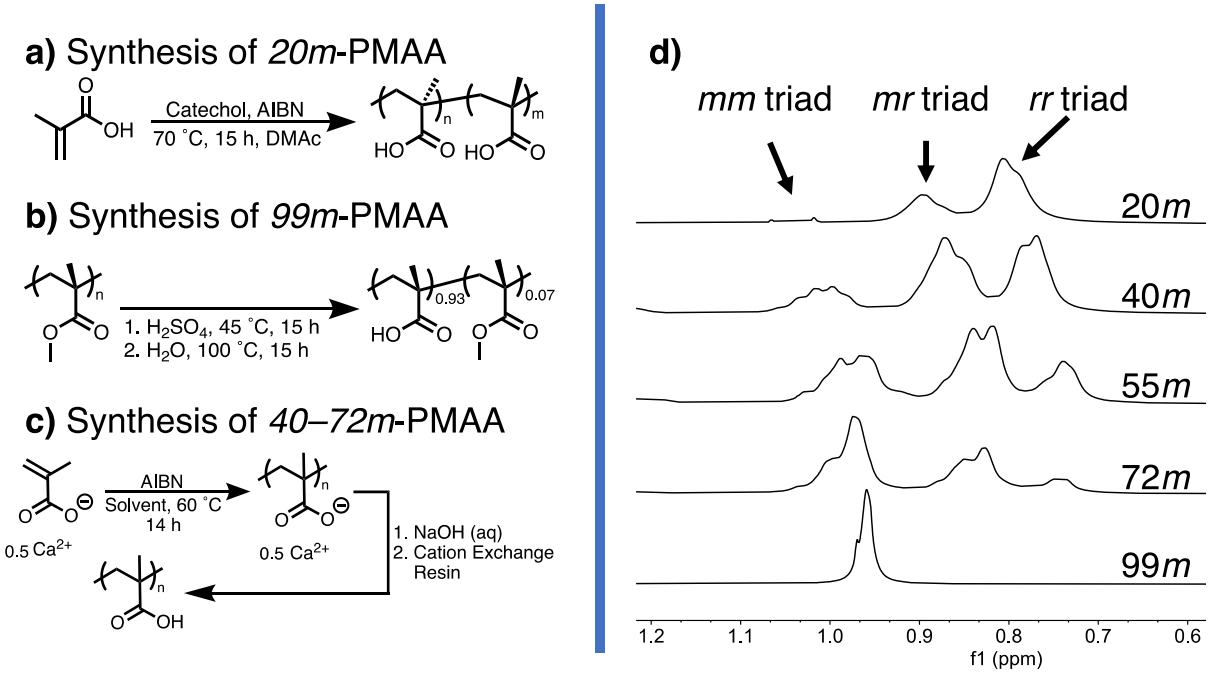

Figure 1. Synthesis of (a) 20*m* PMAA, (b) 99*m* PMAA, (c) 40−72*m* PMAA, and (d) overlaid ^{1}H NMR of the tactic polymer series showing the *mm*, *mr*, and *rr* triads for each polymer sample. The percent *meso* diad for each polymer sample was calculated according to eq S1 using the relative integrations of the peaks corresponding to the *mm*, *mr*, and *rr* triads.

Table 1. Synthesis and Characterization Data of the Tactic PMAA Series

entry	name	monomer	additive	solvent	tacticity[e] (*mm*/*mr*/*rr*)
1	20*m* PMAA[f]	PMAA[a]	catechol[b]	DMAc[c]	5/30/65
2	40*m* PMAA[g]	PMAA-Ca[a]	N/A	DMF[d](1)/water(2)	19/42/39
3	55*m* PMAA[g]	PMAA-Ca[a]	N/A	DMF[d](2)/water(1)	32/45/23
4	72*m* PMAA[g]	PMAA-Ca[a]	N/A	DMF[d]	55/34/11
5	99*m* PMAA[h]	N/A	N/A	N/A	96/3/1

[a]Polymerization conditions: Monomer = 50 mmol, AIBN = 0.1 mmol, reaction temperature = 60 °C, reaction time = 14 h. [b]25 mmol. [c]Dimethylacetamide. [d]Dimethylformamide. [e]Determined by the integrated ratio of the backbone methyl signals in the ^{1}H NMR spectrum (MeOD). [f]Free radical polymerization as previously reported.[46] [g]Free radical polymerization as previously reported.[48] [h]Hydrolysis of commercial isotactic PMMA by H_2SO_4 in water.[47]

metal-binding thermodynamics. Building on previous studies, which often evaluated syndiotactic or isotactic polymers, we synthesized a series of five polymers with systematic variations in tacticity. This expanded series enabled us to produce a more systematic insight into the role of polymer tacticity in REE binding.

RESULTS AND DISCUSSION

To investigate the precise effect of tacticity on the ΔH and ΔS of metal binding, we synthesized PMAA with varied amounts of *m* diads and measured the REE chelation thermodynamics by using isothermal titration calorimetry (ITC). ITC directly measures ΔH, K_a, and the stoichiometry (N) of binding interactions in solution, subsequently enabling calculation of the ΔG and ΔS of the interaction according to eq 1[45]

$$\Delta G = -RT\ln(K_a) = \Delta H - T\Delta S \quad (1)$$

To produce PMAA with varied degrees of stereoregularity, we systematically adjusted the polymerization conditions of methacrylic acid (Figure 1). PMAA rich in *r* diads (syndiotactic) was synthesized via a free-radical polymerization in the presence of catechol. Catechol forms a pseudodivinyl monomer with methacrylic acid, which promotes racemic addition of the monomer during polymerization (Figure 1A).[46] *Isotactic*-PMAA was synthesized by acidic hydrolysis of commercially available *isotactic*-poly(methyl methacrylate) (>99% *m* diad) (Figure 1B).[47] We accessed gradients of PMAA tacticities (40−72% *m* diad) via free-radical polymerization of a PMAA−Ca^{2+} dimer in solvent mixtures with varied polarities (Figure 1C).[48] For each of the resulting polymers, we determined the tacticity by integrating the nuclear magnetic resonance (NMR) peaks corresponding to the *mm*, *mr*, and *rr* triads of the methyl group in the polymer backbone and calculated the percent *m* diads for each polymer according to eq S1 (Table 1, Figures 1D and S1). The M_n of each material was determined by aqueous size-exclusion chromatography and ranged from 89.6 to 386.9 kDa (Figure S2 and Table S1). We previously observed that molecular weight did not have a significant effect on polymer−metal binding thermodynamics in this relatively high molecular weight range and consequently concluded that differences in metal-chelation thermodynamics can be ascribed to the systematical variations in tacticity rather than differences in molecular weight.[49]

Having synthesized a PMAA series with systematically varied tacticity (20*m*−99*m*), we measured the REE−polymer binding thermodynamics with a representative set of REEs (La^{3+}, Nd^{3+},

https://doi.org/10.1021/acs.macromol.3c01163
Macromolecules 2023, 56, 9062−9069

Eu^{3+}, Gd^{3+}, Dy^{3+}, Ho^{3+}, and Lu^{3+}). ITC experiments were conducted by titrating solutions of each REE ion into polymer solutions in a pH 5 HOAc−NaOAc buffer (Figure 2). Control

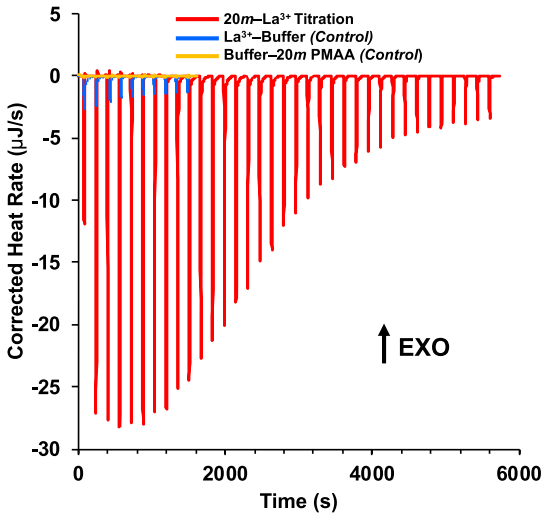

Figure 2. ITC thermogram of a 20*m*−La^{3+} titration (red) overlaid with control titrations (blue and gold).

titrations (buffer into polymer and metal-ion into buffer) were performed to subtract enthalpies that were not the direct result of polymer−REE interactions. Each polymer−REE interaction was endothermic, and we observed relatively large values for $|-T\Delta S|$. These entropy−driven interactions are largely the result of releasing bound water molecules surrounding the polymer and REE ion, consistent with previous observations in both polymer−metal and protein−metal binding thermodynamics.[7,49−55] Interestingly, we observed larger $|\Delta H|$ and $|-T\Delta S|$ values for the more isotactic PMAAs (Figures 3 and 4A,B), with only slight variations in ΔG across the series.

This trend in binding thermodynamics supports our initial hypothesis that tacticity can modulate metal-binding interactions; however, the changes in ΔH and ΔS largely compensated for each other (Figure 4C), producing only modest changes in the binding affinity. This enthalpy−entropy compensation (EEC) is a well-known phenomenon, particularly in biological contexts such as protein−ligand binding, but is less commonly observed in fully synthetic systems.[56−58] The origin of this effect is the subject of considerable discussion in the literature, and it is often thought to depend on the specific system being described.[59] We believe that the EEC observed may be due to multiple factors. First, the lower chain flexibility of *isotactic*-PMAA likely reduces the ability of the polymer to adopt the conformations needed to accommodate metal binding, thereby producing a larger enthalpic penalty. However, the charge screening that occurs upon metal binding to PMAA could potentially enable increased conformational flexibility of the chain, resulting in a higher ΔS, largely compensating for the increase in ΔH. This compensation is likely tied to changes in both the polymer conformation and the solvating water structure. Molecular rigidity in the context of biological macromolecules has previously been connected with EEC, and our results suggest a similar relationship.[60,61] On average, $|-T\Delta S|$ for 99*m* PMAA (the most isotactic material) was 71.8 ± 3.2 kJ mol^{-1}, while $|-T\Delta S|$ for 20*m* PMAA (the most syndiotactic material) was 46.7 ± 2.7 kJ mol^{-1}.

Additionally, changes in water structure are frequently implicated in EEC. In the case of PMAA, the hydration structure is known to change with changing tacticity,[44] and these variations may produce the observed EEC upon metal binding. Our previous research with REE−polymer interactions indicates that differences in ΔS can often be attributed to changes in the water structure surrounding the chelating ligand (the carboxylate).[52] Specifically, we found that upon REE binding the low-entropy (i.e., more ordered) water molecules that are structured by both the carboxylate ligand and REE ion are transferred to the bulk solvent, which produced large positive changes in heat capacity (ΔC_p). To investigate whether the entropy differences observed here could be similarly attributed to water structure, or if they arose primarily from changes in the polymer conformation, we conducted a series of atomistic simulations of PMAA with varying degrees of tacticity. Full details of the computational

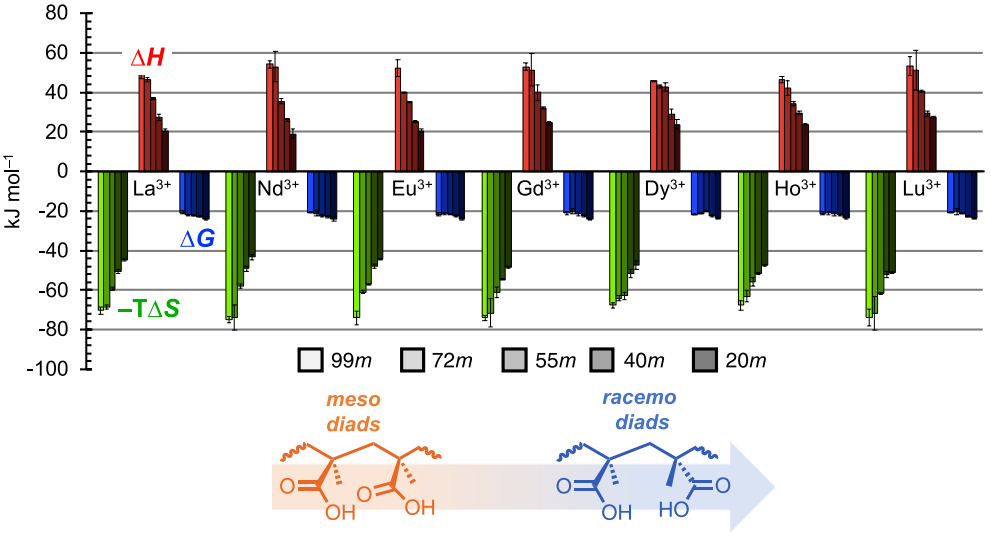

Figure 3. Thermodynamic parameters for REE−PMAA binding. We found that binding became more favorable as the percentage of *m* diad decreased, with both $|\Delta H|$ and $|\Delta S|$ decreasing with decreasing *m* diad content.

https://doi.org/10.1021/acs.macromol.3c01163
Macromolecules 2023, 56, 9062−9069

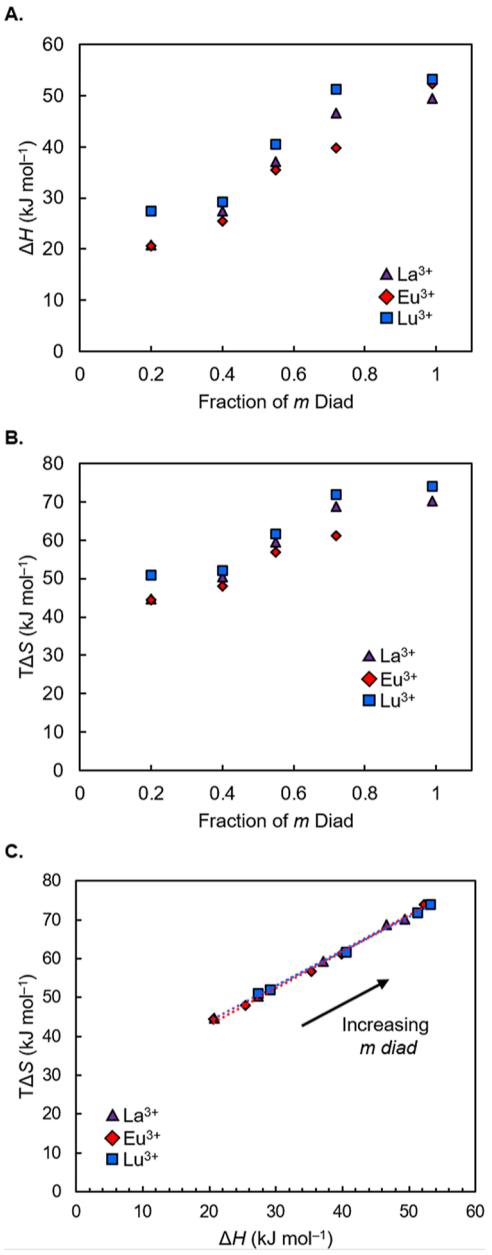

Figure 4. (A) Plot of ΔH dependence on the fraction of *m* diad, (B) $T\Delta S$ dependence on the fraction of *m* diad, and (C) EEC plot. A subset of metal ions (La^{3+}, Eu^{3+}, and Lu^{3+}) is shown for clarity.

methods are included in the Supporting Information. For comparison, we included fully syndiotactic PMAA in these simulations, though this material was not synthesized and thus could not be experimentally evaluated using ITC. Because the polymer chains in the MD simulations are relatively small, we elected to model them in the fully deprotonated state to avoid the possibility that the distribution of protonated repeat units in a partially protonated model might produce significant changes that mask differences arising from variations in tacticity, which is the variable we sought to evaluate (see below).

We quantified the polymer conformational flexibility and water structure surrounding individual polymer chains by computing radial distribution functions (RDFs) (the full data set is provided in the Supporting Information). We had hypothesized that tacticity-driven variations in the number of water molecules displaced during metal binding may account for the observed differences in entropy, but the RDFs comparing the distances between the oxygen atoms in the carboxylates and water molecules ($O(COO^-)-O(H_2O)$) show that the oxygens of the carboxylate groups interact with the same number of water molecules for each polymer in the series and that this is the case both before and after metal ions are introduced in the simulation (Figures S11−S12 and Table S4). This result suggests that the differences between PMAA samples observed experimentally are likely not due to significant differences in displaced water molecules during metal binding, in contrast to our previous work with metal-chelating polyacrylamides.[52] Instead, the increasing stiffness of the polymer chains with increasing percentages of *m* diads could explain the increasing entropic term (Figures 3 and 4B).

We hypothesized that in the absence of REE ions 99*m* PMAA exists in a lower-entropy state in part due to its extended-chain conformation. When metal ions begin to chelate, charge screening along the polymer backbone may enable 99*m* PMAA to access more polymer conformations, thereby producing the large differences in ΔS that we observed across this tacticity series. This hypothesis is partly supported by our simulations (Figures S14 and S15 and Table S4) in that we observe decreased ordering (i.e., a broader peak in the RDF) of water molecules in the second solvation shell around the carbon of the carboxylate groups with increasing *m* diad content only upon introduction of the metal ions. However, this trend is not observed on the backbone−backbone RDFs (Figures S16 and S17 and Table S4), which suggests that the increased flexibility is localized in the pendant carboxylate groups while the rest of the polymer chain remains as rigid as it was prior to the introduction of the metal ions. This hypothesis is also reinforced by the RDF comparing the distance between polymer carboxylates ($C(COO^-)-C(COO^-)$), which shows much greater disorder in the first peak (around 3 Å) with increasing *m* diad content upon the introduction of the ions (Figures S18 and S19).

High amounts of *m* diads also affect the binding stoichiometry, *N* (Table S3). The binding stoichiometry represents the ratio of polymer carboxylates to bound metal ions at saturation. Except for 99*m* PMAA, ITC experiments revealed *N* values of approximately 7−10 for all metals, meaning that at saturation, the molar ratio between polymer carboxylates and REE ions was about 8:1 on average. These values for *N* are slightly higher than those with previously reported materials: for example, on average, *N* for poly(acrylic acid)−REE binding is 5 repeating units per REE ion,[53] while *N* varies between 3 and 5 repeat units of poly(ethyleneimine methylene phosphonate) per REE ion.[49] It is unlikely that all carboxylates are directly participating in metal binding but rather that only a fraction of carboxylates are oriented such that binding is favorable, while the other repeat units adopt conformations that facilitate metal binding at these specific sites. For 99*m* PMAA, the ratio was 15−20 carboxylate repeat units per REE ion. We believe that this outlier is not due to significant changes in binding stoichiometry but rather due to differences in the solubility of the 99*m* PMAA compared to the other polymers in the series.

It is well documented that *iso*-PMAA is insoluble at low degrees of carboxylic acid ionization.[62] Previous experiments have indicated that *iso*-PMAA is a weaker acid than *atactic*-PMAA, resulting from increased charge repulsion upon deprotonation of neighboring carboxylic acid groups on the

https://doi.org/10.1021/acs.macromol.3c01163
Macromolecules 2023, 56, 9062−9069

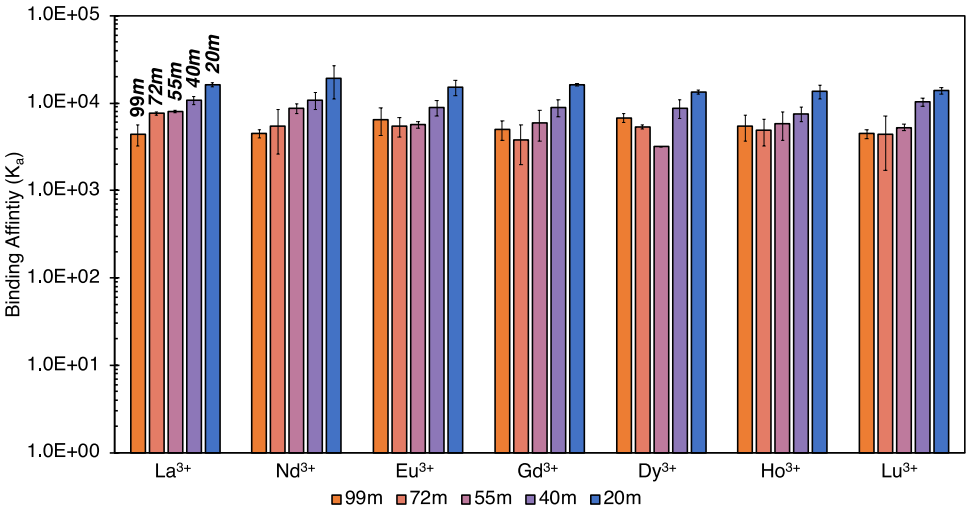

Figure 5. ITC binding affinities as a function of percent *m* diad for REE series. Higher values of K_a indicate the formation of stronger polymer−REE complexes.

same side of the chain in *iso*-PMAA.[63] We hypothesize that the increased binding stoichiometry observed in 99*m* PMAA is the result of the decreased solubility of PMAA in the pH 5 buffer. A polymer with decreased solubility effectively has a lower solution concentration; thus, in the ITC experiment, a lower metal concentration is required to achieve saturation, thereby resulting in higher measured values of *N*. However, the formation of insoluble lanthanide hydroxides above pH 6 precludes performing ITC experiments at a higher pH (i.e., greater carboxylic acid ionization).[64] Furthermore, because the binding affinity for the REE ion is lower for 99*m* PMAA, reducing the concentration of this polymer in solution is insufficient to obtain a sigmoidal titration curve.[65] The ΔH, ΔG, and ΔS parameters are determined independently of the molar ratio in an ITC experiment, thus the effect of the polymer solubility on determining these parameters is negligible.[45] Additionally, we previously investigated polymer aggregation as a function of metal-ion concentration using dynamic light scattering (DLS) at concentrations directly correlated with our ITC data.[49] DLS experiments indicated that the polymer−metal complexation immediately results in the formation of large aggregates; however, despite aggregation, the shape of the ITC curve remains sigmoidal.

The binding affinity (K_a) reflects the strength of the REE−PMAA complexes in solution. In some metal-binding applications, K_a must be modulated to balance efficient chelation with the ability to release metals from the polymer. Thus, K_a can dictate the potential utility of these materials in metal-chelation applications. The average K_a for these REE−PMAA interactions varied between 4.4×10^3 and 1.6×10^4. In general, we observed higher values of K_a for 20*m* PMAA than for the other polymers (Figure 5), though the differences across the series are relatively small due to EEC. For example, K_a for La^{3+} was $4.4 \times 10^3 \pm 1.2$ for 99*m* PMAA and $1.62 \times 10^4 \pm 0.08$ for 20*m* PMAA. Higher values of K_a indicate the formation of stronger polymer−REE complexes.

To provide further insight into these K_a trends, we calculated Eu^{3+}−polymer interaction energies from our MD simulations (Table S5). More specifically, we selected the Eu^{3+} ions that were closest to the polymer (within 5 Å as shown in Figure S20) and computed individual interaction energies with the polymer in the absence of water. From these calculations, we see that the interaction between individual ions and the polymer is first weakened as the percentage of *m* diads increases from 0 (syndiotactic) to 55*m*, then strengthened going from 55*m* to fully isotactic. The interaction energy calculated from our simulations roughly correlates with the binding affinities in Figure 5, where we observe a similar trend for the Eu^{3+} ions specifically. However, water plays a decisive role in metal binding in solution, so these calculations in the absence of water capture only one facet of the polymer−metal interaction.

Taken together, these experimental and computational results suggest a multifaceted role of tacticity in polymer−metal binding. Polymer conformation unquestionably plays a role, as has been previously observed both experimentally and in simulations in previous publications,[20,52,54] but perturbations in water structure are likely central in the changes in thermodynamics we observed. These two factors, however, are challenging to deconvolute, as changes in polymer conformation produce changes in water structure with both ultimately influencing polymer−metal interactions. The complex interplay between these two factors is perhaps inherently compensatory with regard to overall binding thermodynamics; e.g., conformational changes that enhance enthalpic interactions with ions and water also reduce entropy.

CONCLUSIONS

In conclusion, we synthesized a series of PMAA copolymers with varied degrees of stereoregularity (99*m*−20*m*) to measure the effect of polymer tacticity on REE chelation thermodynamics using ITC. We found that ΔH increased as the *m* diad content increased (i.e., more isotactic polymers). Furthermore, the increase in ΔH was largely offset by an increase in ΔS, which resulted in a near-uniform ΔG for this series of polymers, a clear example of EEC in a nonbiological system. Molecular dynamics simulations suggested that the polymer stereoregularity controls the conformation of the chelating ligands, ultimately influencing the thermodynamics of metal binding. This work lays the foundation for a broader consideration of polymer stereostructure as new and increasingly effective metal-chelating materials are developed. However, polymer stereostructure, chelating ligand conformation, and polymer desolvation effects are just a few facets of the

https://doi.org/10.1021/acs.macromol.3c01163
Macromolecules 2023, 56, 9062−9069

polymer−metal interaction. Deconvoluting and ultimately controlling these individual effects remains an ongoing challenge.

■ ASSOCIATED CONTENT

Supporting Information

The Supporting Information is available free of charge at https://pubs.acs.org/doi/10.1021/acs.macromol.3c01163.

Experimental and computational procedures, NMR spectra, and parameters for ITC analysis (PDF)

■ AUTHOR INFORMATION

Corresponding Author

Michael D. Schulz − *Department of Chemistry and Macromolecules Innovation Institute, Virginia Tech, Blacksburg, Virginia 24061, United States;* orcid.org/0000-0001-8499-6025; Email: mdschulz@vt.edu

Authors

William R. Archer − *Department of Chemistry and Macromolecules Innovation Institute, Virginia Tech, Blacksburg, Virginia 24061, United States;* orcid.org/0000-0002-6326-6602

Taoyi Chen − *Department of Chemistry and Macromolecules Innovation Institute, Virginia Tech, Blacksburg, Virginia 24061, United States*

Valerie Vaissier Welborn − *Department of Chemistry and Macromolecules Innovation Institute, Virginia Tech, Blacksburg, Virginia 24061, United States;* orcid.org/0000-0003-0834-4441

Complete contact information is available at: https://pubs.acs.org/10.1021/acs.macromol.3c01163

Notes

The authors declare no competing financial interest.

■ ACKNOWLEDGMENTS

The authors wish to acknowledge the Virginia Tech Department of Chemistry Faculty Start-up funds for financial support. This work was supported by the U.S. Department of Energy, Office of Science, Office of Basic Energy Sciences, under award number DE-SC0023035. The simulation experiments were also supported by GlycoMIP, a National Science Foundation Materials Innovation Platform funded through Cooperative Agreement DMR-1933525. The authors also wish to thank Prof. Adrian Figg for assistance in collecting the aqueous SEC data of the polymer samples.

■ REFERENCES

(1) Nguyen, H. V. T.; Jiang, Y.; Mohapatra, S.; Wang, W.; Barnes, J. C.; Oldenhuis, N. J.; Chen, K. K.; Axelrod, S.; Huang, Z.; Chen, Q.; Golder, M. R.; Young, K.; Suvlu, D.; Shen, Y.; Willard, A. P.; Hore, M. J. A.; Gómez-Bombarelli, R.; Johnson, J. A. Bottlebrush polymers with flexible enantiomeric side chains display differential biological properties. *Nat. Chem.* **2022**, *14* (1), 85−93.

(2) Popowski, Y.; Lu, Y.; Coates, G. W.; Tolman, W. B. Stereocomplexation of Stereoregular Aliphatic Polyesters: Change from Amorphous to Semicrystalline Polymers with Single Stereocenter Inversion. *J. Am. Chem. Soc.* **2022**, *144* (18), 8362−8370.

(3) Knutson, P. C.; Teator, A. J.; Varner, T. P.; Kozuszek, C. T.; Jacky, P. E.; Leibfarth, F. A. Brønsted Acid Catalyzed Stereoselective Polymerization of Vinyl Ethers. *J. Am. Chem. Soc.* **2021**, *143* (40), 16388−16393.

(4) Warren, J. L.; Dykeman-Bermingham, P. A.; Knight, A. S. Controlling Amphiphilic Polymer Folding beyond the Primary Structure with Protein-Mimetic Di(Phenylalanine). *J. Am. Chem. Soc.* **2021**, *143* (33), 13228−13234.

(5) O'Brien, E. P.; Brooks, B. R.; Thirumalai, D. Effects of pH on Proteins: Predictions for Ensemble and Single-Molecule Pulling Experiments. *J. Am. Chem. Soc.* **2012**, *134* (2), 979−987.

(6) Jung, Y.; Bayley, H.; Movileanu, L. Temperature-Responsive Protein Pores. *J. Am. Chem. Soc.* **2006**, *128* (47), 15332−15340.

(7) Cotruvo, J. A.; Featherston, E. R.; Mattocks, J. A.; Ho, J. V.; Laremore, T. N. Lanmodulin: A Highly Selective Lanthanide-Binding Protein from a Lanthanide-Utilizing Bacterium. *J. Am. Chem. Soc.* **2018**, *140* (44), 15056−15061.

(8) Quinn, M. K.; James, S.; McManus, J. J. Chemical Modification Alters Protein−Protein Interactions and Can Lead to Lower Protein Solubility. *J. Phys. Chem. B* **2019**, *123* (20), 4373−4379.

(9) Karasz, F. E.; MacKnight, W. J. The Influence of Stereoregularity on the Glass Transition Temperatures of Vinyl Polymers. *Macromolecules* **1968**, *1* (6), 537−540.

(10) Schneider, B.; Štokr, J.; Dirlikov, S.; Mihailov, M. Conformational Structure and Vibrational Spectra of Poly(methyl methacrylate) and of Its Models. *Macromolecules* **1971**, *4* (6), 715−718.

(11) Burfield, D. R.; Doi, Y. Differential scanning calorimetry characterization of polypropylene. Dependence of Tg on polymer tacticity and molecular weight. *Macromolecules* **1983**, *16* (4), 702−704.

(12) Beaucage, G.; Stein, R. S.; Hashimoto, T.; Hasegawa, H. Tacticity effects on polymer blend miscibility. *Macromolecules* **1991**, *24* (11), 3443−3448.

(13) Jones, T. D.; Chaffin, K. A.; Bates, F. S.; Annis, B. K.; Hagaman, E. W.; Kim, M.-H.; Wignall, G. D.; Fan, W.; Waymouth, R. Effect of Tacticity on Coil Dimensions and Thermodynamic Properties of Polypropylene. *Macromolecules* **2002**, *35* (13), 5061−5068.

(14) Huang, C.-L.; Chen, Y.-C.; Hsiao, T.-J.; Tsai, J.-C.; Wang, C. Effect of Tacticity on Viscoelastic Properties of Polystyrene. *Macromolecules* **2011**, *44* (15), 6155−6161.

(15) Samal, S.; Thompson, B. C. Influence of Alkyl Chain Spacer Length on the Charge Carrier Mobility of Isotactic Poly(N-carbazolylalkyl acrylates). *ACS Macro Lett.* **2021**, *10* (6), 720−726.

(16) Biroš, J.; Larina, T.; Trekoval, J.; Pouchlý, J. Dependence of the glass transition temperature of poly (methyl methacrylates) on their tacticity. *J. Colloid Polym. Sci.* **1982**, *260* (1), 27−30.

(17) Maurer, J. J.; Eustace, D. J.; Ratcliffe, C. T. Thermal characterization of poly(acrylic acid). *Macromolecules* **1987**, *20* (1), 196−202.

(18) Karasz, F. E.; Bair, H. E.; O'Reilly, J. M. Thermal Properties of Atactic and Isotactic Polystyrene. *J. Phys. Chem.* **1965**, *69* (8), 2657−2667.

(19) Hriberšek, P.; Kogej, K. Tacticity and Counterion Modulated Temperature Response of Weak Polyelectrolytes: The Case of Poly(methacrylic acid) Stereoisomers in Aqueous Solutions. *Macromolecules* **2019**, *52* (18), 7028−7041.

(20) Morcellet, M. Effect of tacticity on the association of poly(methacrylic acid) with divalent metal ions. *J. Polym. Sci. B Polym. Lett.* **1985**, *23*, 99−102.

(21) Archer, W. R.; Hall, B. A.; Thompson, T. N.; Wadsworth, O. J.; Schulz, M. D. Polymer sequestrants for biological and environmental applications. *Polym. Int.* **2019**, *68* (7), 1220−1237.

(22) Popwell, S. J.; Schulz, M. D.; Wagener, K. B.; Batich, C. D.; Milner, R. J.; Lagmay, J.; Bolch, W. E. Synthesis of Polymeric Phosphonates for Selective Delivery of Radionuclides to Osteosarcoma. *Cancer Biother. Rad.* **2014**, *29* (7), 273−282.

(23) Qian, J.; Sullivan, B.; Peterson, S.; Berkland, C. Nonabsorbable Iron Binding Polymers Prevent Dietary Iron Absorption for the Treatment of Iron Overload. *ACS Macro Lett.* **2017**, *6*, 350−353.

(24) Archer, W. R.; Iftekhar, N.; Fiorito, A.; Winn, S. A.; Schulz, M. D. Synthesis of Phosphonated Polymer Resins for the Extraction of Rare-Earth Elements. *ACS Appl. Polym. Mater.* **2022**, *4* (4), 2506−2512.

(25) Mitchell, L. A.; Holliday, B. J. Polymeric Materials for the Separation of f-Elements Utilizing Carbamoylmethylphosphine Oxide Chelating Ligands. *ACS Macro Lett.* **2016**, *5* (10), 1100−1103.
(26) Bashiri, A.; Nikzad, A.; Maleki, R.; Asadnia, M.; Razmjou, A. Rare Earth Elements Recovery Using Selective Membranes via Extraction and Rejection. *Membranes* **2022**, *12* (1), 80.
(27) Jordens, A.; Cheng, Y. P.; Waters, K. E. A review of the beneficiation of rare earth element bearing minerals. *Miner. Eng.* **2013**, *41*, 97−114.
(28) Massari, S.; Ruberti, M. Rare earth elements as critical raw materials: Focus on international markets and future strategies. *Resour. Pol.* **2013**, *38* (1), 36−43.
(29) Liu, T.; Johnson, K. R.; Jansone-Popova, S.; Jiang, D.-e. Advancing Rare-Earth Separation by Machine Learning. *JACS Au* **2022**, *2* (6), 1428−1434.
(30) Guo, Y.; Zhang, X.; Sun, X.; Kong, D.; Han, M.; Wang, X. Nanoadsorbents Based on NIPAM and Citric Acid: Removal Efficacy of Heavy Metal Ions in Different Media. *ACS Omega* **2019**, *4* (10), 14162−14168.
(31) Gomes Rodrigues, D.; Monge, S.; Pellet-Rostaing, S.; Dacheux, N.; Bouyer, D.; Faur, C. A new carbamoylmethylphosphonic acid-based polymer for the selective sorption of rare earth elements. *Chem. Eng. J.* **2019**, *371*, 857−867.
(32) Kołodyńska, D. Diphonix Resin® in sorption of heavy metal ions in the presence of the biodegradable complexing agents of a new generation. *Chem. Eng. J.* **2010**, *159*, 27−36.
(33) Okamoto, S.; Vyprachticky, D.; Furuya, H.; Abe, A.; Okamoto, Y. Ion Binding Properties of Polycarboxylates Using Terbium(III) as a Fluorescent Probe: Viscosities and Coordinated Water Molecules in Polycarboxylate−Terbium(III) Complexes in Aqueous Solutions. *Macromolecules* **1996**, *29* (10), 3511−3514.
(34) Kogej, K.; Fonseca, S. M.; Rovisco, J.; Azenha, M. E.; Ramos, M. L.; Seixas de Melo, J. S.; Burrows, H. D. Understanding the Interaction between Trivalent Lanthanide Ions and Stereoregular Polymethacrylates through Luminescence, Binding Isotherms, NMR, and Interaction with Cetylpyridinium Chloride. *Langmuir* **2013**, *29* (47), 14429−14437.
(35) Hriberšek, P.; Kogej, K. Effect of Multivalent Cations on Intermolecular Association of Isotactic and Atactic Poly(Methacrylic Acid) Chains in Aqueous Solutions. *Polymers* **2019**, *11* (4), 605.
(36) Schneider, B.; Kabeláč, M. Stereochemistry of Binding of Metal Cations and Water to a Phosphate Group. *J. Am. Chem. Soc.* **1998**, *120* (1), 161−165.
(37) Carrabine, J. A.; Sundaralingam, M. Stereochemistry of Nucleic Acids and Their Constituents. VIII. Metal Binding Studies. Crystal Structure of a Guanine-Copper Chloride Complex, a Trigonal-Bipyramidally Coordinated Copper. *J. Am. Chem. Soc.* **1970**, *92* (2), 369−371.
(38) Qian, J.; Berkland, C. Conformational Stability Effect of Polymeric Iron Chelators. *iScience* **2019**, *21*, 124−134.
(39) Fortuna, S.; Fogolari, F.; Scoles, G. Chelating effect in short polymers for the design of bidentate binders of increased affinity and selectivity. *Sci. Rep.* **2015**, *5* (1), 15633.
(40) Flory, P. J. *Statistical Mechanics of Chain Molecules*. Repr. ed. with Corrections/ed.; Hanser Publishers; Distributed in the U.S.A. by Oxford University Press: Munich; New York, 1989.
(41) Gupta, A. K. Combined Salt Concentration and Degree-of-Ionization Effect on the Structure of Poly(methacrylic acid) in Aqueous Solutions as Revealed by Molecular Dynamics Simulations. *Ind. Eng. Chem. Res.* **2021**, *60* (13), 4806−4819.
(42) Wang, Z.-G. 50th Anniversary Perspective: Polymer Conformation—A Pedagogical Review. *Macromolecules* **2017**, *50* (23), 9073−9114.
(43) Xu, Y.; Wang, Z.-G. Coil-to-Globule Transition in Polymeric Solvents. *Macromolecules* **2021**, *54* (23), 10984−10993.
(44) Gupta, A. K.; Natarajan, U. Tacticity effects on conformational structure and hydration of poly-(methacrylic acid) in aqueous solutions-a molecular dynamics simulation study. *Mol. Simul.* **2016**, *42* (9), 725−736.
(45) Archer, W. R.; Schulz, M. D. Isothermal titration calorimetry: practical approaches and current applications in soft matter. *Soft Matter* **2020**, *16* (38), 8760−8774.
(46) Saito, Y.; Saito, R. Synthesis of syndiotactic poly(methacrylic acid) by free-radical polymerization of the pseudo-divinyl monomer formed with methacrylic acid and catechol. *J. Appl. Polym. Sci.* **2013**, *128* (6), 3528−3533.
(47) Semen, J.; Lando, J. B. The Acid Hydrolysis of Isotactic and Syndiotactic Poly(methyl methacrylate). *Macromolecules* **1969**, *2* (6), 570−575.
(48) Kaneko, Y.; Iwakiri, N.; Sato, S.; Kadokawa, J.-i. Stereospecific Free-Radical Polymerization of Methacrylic Acid Calcium Salt for Facile Preparation of Isotactic-Rich Polymers. *Macromolecules* **2008**, *41* (2), 489−492.
(49) Archer, W. R.; Fiorito, A.; Heinz-Kunert, S. L.; MacNicol, P. L.; Winn, S. A.; Schulz, M. D. Synthesis and Rare-Earth-Element Chelation Properties of Linear Poly(ethylenimine methylenephosphonate). *Macromolecules* **2020**, *53* (6), 2061−2068.
(50) Nishide, H.; Izushi, T.; Arai, H.; Yoshioka, N.; Tsuchida, E. Complexation Constants of Lanthanide Ions with Poly(Methacrylic Acid) and its Copolymers. *J. Macromol. Sci., Chem.* **1987**, *24* (3−4), 343−351.
(51) Ferrie, L.; Arrambide, C.; Darcos, V.; Prelot, B.; Monge, S. Synthesis and evaluation of functional carboxylic acid based poly(εCL-st-αCOOHεCL)-b-PEG-b-poly(εCL-st-αCOOHεCL) copolymers for neodymium and cerium complexation. *React. Funct. Polym.* **2022**, *171*, 105157.
(52) Archer, W. R.; Gallagher, C. M. B.; Vaissier Welborn, V.; Schulz, M. D. Exploring the role of polymer hydrophobicity in polymer−metal binding thermodynamics. *Phys. Chem. Chem. Phys.* **2022**, *24* (6), 3579−3585.
(53) Archer, W. R.; Thompson, T. N.; Schulz, M. D. Effect of Copolymer Structure on Rare-Earth-Element Chelation Thermodynamics. *Macromol. Rapid Commun.* **2021**, *42* (8), 2000614.
(54) Welborn, V. V.; Archer, W. R.; Schulz, M. D. Characterizing Ion-Polymer Interactions in Aqueous Environment with Electric Fields. *J. Chem. Inf. Model.* **2023**, *63* (7), 2030−2036.
(55) Mattocks, J. A.; Cotruvo, J. A.; Deblonde, G. J. P. Engineering lanmodulin's selectivity for actinides over lanthanides by controlling solvent coordination and second-sphere interactions. *Chem. Sci.* **2022**, *13* (20), 6054−6066.
(56) Peccati, F.; Jiménez-Osés, G. Enthalpy−Entropy Compensation in Biomolecular Recognition: A Computational Perspective. *ACS Omega* **2021**, *6* (17), 11122−11130.
(57) Chodera, J. D.; Mobley, D. L. Entropy-Enthalpy Compensation: Role and Ramifications in Biomolecular Ligand Recognition and Design. *Annu. Rev. Biophys.* **2013**, *42* (1), 121−142.
(58) Gilli, P.; Ferretti, V.; Gilli, G.; Borea, P. A. Enthalpy-entropy compensation in drug-receptor binding. *J. Phys. Chem.* **1994**, *98* (5), 1515−1518.
(59) Fox, J. M.; Zhao, M.; Fink, M. J.; Kang, K.; Whitesides, G. M. The Molecular Origin of Enthalpy/Entropy Compensation in Biomolecular Recognition. *Annu. Rev. Biophys.* **2018**, *47* (1), 223−250.
(60) Vargas-Lara, F.; Starr, F. W.; Douglas, J. F. Molecular rigidity and enthalpy−entropy compensation in DNA melting. *Soft Matter* **2017**, *13* (44), 8309−8330.
(61) Krishnamurthy, V. M.; Bohall, B. R.; Semetey, V.; Whitesides, G. M. The Paradoxical Thermodynamic Basis for the Interaction of Ethylene Glycol, Glycine, and Sarcosine Chains with Bovine Carbonic Anhydrase II: An Unexpected Manifestation of Enthalpy/Entropy Compensation. *J. Am. Chem. Soc.* **2006**, *128* (17), 5802−5812.
(62) van den Bosch, E.; Keil, Q.; Filipcsei, G.; Berghmans, H.; Reynaers, H. Structure Formation in Isotactic Poly(methacrylic acid). *Macromolecules* **2004**, *37* (26), 9673−9675.
(63) Costantino, L.; Crescenzi, V.; Quadrifoglio, F.; Vitagliano, V. Influence of stereoregularity on binding of counterions by poly-(methacrylic acid). *J. Polym. Sci. 2 Polym. Phys.* **1967**, *5* (4), 771−780.

https://doi.org/10.1021/acs.macromol.3c01163
Macromolecules 2023, 56, 9062−9069

(64) Cawthray, J. F.; Creagh, A. L.; Haynes, C. A.; Orvig, C. Ion Exchange in Hydroxyapatite with Lanthanides. *Inorg. Chem.* **2015**, *54* (4), 1440−1445.
(65) Turnbull, W. B.; Daranas, A. H. On the Value of c: Can Low Affinity Systems Be Studied by Isothermal Titration Calorimetry? *J. Am. Chem. Soc.* **2003**, *125* (48), 14859−14866.

https://doi.org/10.1021/acs.macromol.3c01163
Macromolecules 2023, 56, 9062−9069